

Infrared Spectroscopy Studies of Platinum Salts Containing Tetracyanoplatinate(II). Evidence for Strong Hydrogen-Bonding Interactions in “Vapochromic” Environmental Sensor Materials

Christopher L. Exstrom,[†] Marie K. Pomije, and Kent R. Mann*

Department of Chemistry, University of Minnesota, Minneapolis, Minnesota 55455-0431

Received December 5, 1997

We have studied the sorption of volatile organic compounds (VOCs) by $[(n\text{-C}_4\text{H}_9)_4\text{N}]_2[\text{Pt}(\text{CN})_4]$ and $[\text{Pt}(p\text{-CN-C}_6\text{H}_4\text{-C}_{10}\text{H}_{21})_4][\text{Pt}(\text{CN})_4]$ with FTIR spectroscopy. The data indicate a strong correlation exists between $\nu(\text{CN})$ stretching frequencies in the $[\text{Pt}(\text{CN})_4]^{2-}$ ions and the hydrogen bonding ability of the VOC (as expressed by Abraham's α values). The $\nu(\text{CN})$ stretching frequencies for each salt with sorbed VOC indicate that similar VOC-material interactions are present in both. The correlation of the IR data for $[\text{Pt}(p\text{-CN-C}_6\text{H}_4\text{-C}_{10}\text{H}_{21})_4][\text{Pt}(\text{CN})_4]$ with the previously reported NIR data was only successful for solvents with $\alpha > 0.15$. These results suggest that vapochromic shifts in the electronic transitions of $[\text{Pt}(p\text{-CN-C}_6\text{H}_4\text{-C}_{10}\text{H}_{21})_4][\text{Pt}(\text{CN})_4]$ result not only from H-bonds between the VOC and $[\text{Pt}(\text{CN})_4]^{2-}$ but also from one or more additional mechanisms that are most important for solvents with low H-bond donor character ($\alpha < 0.15$).

Introduction

The design of chemical sensor systems is an important area of research due to the growing need to detect and identify volatile organic compounds (VOCs) in the environment.¹ A typical sensor system consists of a chemically sensitive layer and a transducer device.² While data acquisition and analysis instrumentation for various transducers are relatively advanced, well-characterized model systems for the chemically sensitive layers are still needed.³

We are studying promising chemically sensitive layers that are based on square planar d^8 platinum complexes.⁴ These complexes are robust and form intensely colored solid-state materials that respond spectroscopically to the sorption of a wide range of VOCs. Previously, we reported that significant interactions between sorbed guest molecules and cyanide ligands in solid-state $[\text{Pt}$ -

$(p\text{-CN-C}_6\text{H}_4\text{-C}_{10}\text{H}_{21})_4][\text{M}(\text{CN})_4]$ ($\text{M} = \text{Pd}, \text{Pt}$) produce shifts in the $\nu(\text{CN})$ stretching frequencies as well as changes in the UV-vis or near-infrared (NIR) spectra of these solids. Seminal studies of this type were reported many years ago for the irreversible solid/gas adducts formed between BF_3 and metal complexes containing cyanide ligands.⁵ Strong interactions between BF_3 molecules and the nitrogen lone pairs cause an increase in $\nu(\text{CN})$. These studies showed that the BF_3/CN^- interactions did not dramatically affect metal-centered $d-d$ electronic transitions, but metal-to-ligand charge-transfer transitions present were very sensitive to the formation of the Lewis acid adducts. These reports suggest that in the solid state cyanide ligands offer sites that can interact with guest molecules to trigger “vapochromic”^{4a} shifts in the infrared and/or electronic absorption spectra.

In this work, we report IR studies of VOC vapor sorption by $[(n\text{-C}_4\text{H}_9)_4\text{N}]_2[\text{Pt}(\text{CN})_4]$ and $[\text{Pt}(p\text{-CN-C}_6\text{H}_4\text{-C}_{10}\text{H}_{21})_4][\text{Pt}(\text{CN})_4]$. We also compare the interaction of VOCs with the stacked double-complex salt vs the unstacked $[(n\text{-C}_4\text{H}_9)_4\text{N}]_2[\text{Pt}(\text{CN})_4]$. The correlation between the cyanide stretching frequency and the α value (a H-bonding parameter) of the VOC is discussed.

Experimental Section

General Considerations. $[\text{Pt}(p\text{-CN-C}_6\text{H}_4\text{-C}_{10}\text{H}_{21})_4][\text{Pt}(\text{CN})_4]$ was prepared as previously reported.^{4b} $[(n\text{-C}_4\text{H}_9)_4\text{N}]_2[\text{Pt}(\text{CN})_4]$ was prepared from $[(n\text{-C}_4\text{H}_9)_4\text{N}]\text{Br}$ (Aldrich) and $\text{K}_2[\text{Pt}(\text{CN})_4]$ (Strem) as previously reported.⁶ All solvents used

* To whom correspondence should be addressed.

[†] Current address: Department of Chemistry, University of Nebraska-Kearney, Kearney, NE 68849-1150.

(1) A literature search produced several thousand references on the general topic of sensors for the period of 1991–1996. For example, see: (a) Persaud, K.; Dodd, G. H. *Nature (London)* **1982**, *299*, 352. (b) Shurmer, H. V. *Anal. Proc. Inc. Anal. Comm.* **1994**, *31*, 39. (c) The U.S. EPA Environmental Technology Initiative for FY 1994 included monitoring VOCs as a critical need.

(2) (a) Rabolt, J. F.; Santo, R.; Schlotter, N. E.; Swalen, J. D. *IBM J. Res. Dev.* **1982**, *26*, 209. (b) Yang, L.; Saavedra, S. S.; Armstrong, N. R.; Hayes, J. *Anal. Chem.* **1994**, *66*, 1254. (c) Mirkin, C. A.; Valentine, J. R.; Ofer, D.; Hickman, J. J.; Wrighton, M. S. *ACS Symp. Ser.* **1992**, *487*, 218. (d) Hillman, A. R.; Loveday, D. C.; Swann, M. J.; Bruckenstein, S.; Wilde, C. P. *ACS Symp. Ser.* **1992**, *487*, 150. (e) Zellers, E. T.; Zhang, G. Z. *Anal. Chem.* **1992**, *64*, 1277. (f) Szmazinski, H.; Lakowicz, J. R. *ACS Symp. Ser.* **1993**, *538*, 196. (g) DeQuan, L.; Buscher, C. T.; Swanson, B. I. *Chem Mater.* **1994**, *6*, 803.

(3) Dickert, F. L.; Haunschild, A. *Adv. Mater.* **1993**, *5*, 887.

(4) (a) Exstrom, C. L.; Sowa, J. R.; Daws, C. A.; Janzen, D. E.; Mann, K. R. *Chem. Mater.* **1995**, *7*, 15. (b) Daws, C. A.; Exstrom, C. L.; Sowa, J. R.; Mann, K. R. *Chem. Mater.* **1997**, *9*, 363.

(5) (a) Shriver, D. F. *J. Am. Chem. Soc.* **1963**, *85*, 1405–1408. (b) Shriver, D. F. *J. Am. Chem. Soc.* **1962**, *84*, 4610. (c) Schilt, A. A. *J. Am. Chem. Soc.* **1960**, *82*, 3000. (d) Hammer, N. K.; Orgel, L. E. *Nature* **1961**, *190*, 439. (e) Schilt, A. A. *J. Am. Chem. Soc.* **1960**, *82*, 5779. (6) Mason, W. R.; Gray, H. B. *J. Am. Chem. Soc.* **1968**, *90*, 5721.

Table 1. Infrared $\nu(\text{CN})$ Stretching Frequencies for $[(n\text{-C}_4\text{H}_9)_4\text{N}]_2[\text{Pt}(\text{CN})_4]$ (1) and $[\text{Pt}(p\text{-CN-C}_6\text{H}_4\text{-C}_{10}\text{H}_{21})_4][\text{Pt}(\text{CN})_4]$ (2) upon Exposure to Solvents (pK_a , Gas-Phase Acidity, and Hydrogen-Bonding Ability Values for Each Solvent Are Listed)

VOC	$\nu(\text{CN})$ for 1 ^a	$\nu(\text{CN})$ for 2 ^a	pK_a ^b	gas phase acidity ^c	α ^d
none	2118	2125			
1 water	2118	2125	15.74	1635	0.82
2 hexanes	2118	2125	52 est. ^e	1761 est. ^e	0.00
3 acetone	2118	2126	20	1544	0.04
4 carbon tetrachloride	2118	2126			0.00
5 diethyl ether	2118	2126			0.00
6 benzene	2119	2126	43	1677	0.00
7 dimethyl sulfoxide	2120	<i>f</i>	33	1563	0.00
8 dichloromethane	2121	2127		1567	0.10
9 acetonitrile	2122	2127	25	1560	0.07
10 chloroform	2122	2127, 2132	15	1494	0.15
11 isopropyl alcohol	<i>f</i>	2128, 2135	16.48	1571	0.33
12 methanol- <i>d</i> ₄	2128	2128, 2138			
13 ethanol	2129	2128, 2136	15.85	1582	0.37
14 methanol	2130	2128, 2138	15.2	1597	0.43
15 2,2,2-trifluoroethanol	2136	2130, 2140	12.37	1514	0.57
16 glacial acetic acid	2143	2131, 2142	4.76	1457	0.61
17 88% formic acid	2148	2130, 2144	3.77	1445	0.75
18 concentrated hydrochloric acid	2156	<i>g</i>	-7	1395	

^a In cm^{-1} . ^b In water, see ref 10. ^c In kJ/mol , see ref 11. ^d See ref 12. ^e Estimated value based on ethane. ^f Not determined. ^g Nonreversible.

in the IR studies were ACS reagent grade and used as received after drying over molecular sieves.

Instrumental Methods. Infrared absorption spectra were obtained by an attenuated total reflectance (ATR) method with a Nicolet Magna-IR System 550 spectrometer, equipped with a ZnSe trough HATR cell from PIKE Technologies. Data were processed using OMNIC version 1.2 software. Sample films were coated on the ZnSe crystal from either a CH_2Cl_2 solution, diethyl ether suspension, or hexane suspension. Films of insoluble double-complex salts were washed with acetone prior to spectral studies to remove impurities and decomposition products. All traces of the acetone wash were removed in a stream of dry nitrogen until no evidence of acetone in the IR spectrum was observed. VOC vapor was admitted to the film on the ATR crystal by placing a beaker containing the solvent on the ZnSe crystal mount. After the VOC was added to the beaker, the film and crystal mount were covered; typically, numerous spectra were recorded before and after equilibrium vapor pressure of the solvent was established in the headspace above the ATR crystal.

Results and Discussion

Pt(II) bonding to $p\text{-CN-C}_6\text{H}_4\text{-C}_{10}\text{H}_{21}$ shifts the strong isocyanide CN stretching frequency from 2130 cm^{-1} for the free ligand to 2259 cm^{-1} . This value is consistent with those previously reported for $[\text{Pt}(\text{CNR})_4]^{2+}$ complexes.⁷ The cyanide CN stretching frequency for $[\text{Pt}(p\text{-CN-C}_6\text{H}_4\text{-C}_{10}\text{H}_{21})_4][\text{Pt}(\text{CN})_4]$ (2125 cm^{-1}) is close to that observed for the $[(n\text{-C}_4\text{H}_9)_4\text{N}]_2[\text{Pt}(\text{CN})_4]$ precursor (2118 cm^{-1}). The frequency difference may be due to effective delocalization of charge along the Pt–Pt stack in the double-complex salt.

Exposing $[\text{Pt}(p\text{-CN-C}_6\text{H}_4\text{-C}_{10}\text{H}_{21})_4][\text{Pt}(\text{CN})_4]$ or $[(n\text{-C}_4\text{H}_9)_4\text{N}]_2[\text{Pt}(\text{CN})_4]$ solid-state films to most solvent vapors results in $\nu(\text{CN})$ shifts toward higher energy (Table 1). Figure 1a,b shows a series of IR absorption spectra for the sorption of CH_3OH vapor by films of $[(n\text{-C}_4\text{H}_9)_4\text{N}]_2[\text{Pt}(\text{CN})_4]$ and $[\text{Pt}(p\text{-CN-C}_6\text{H}_4\text{-C}_{10}\text{H}_{21})_4][\text{Pt}(\text{CN})_4]$.

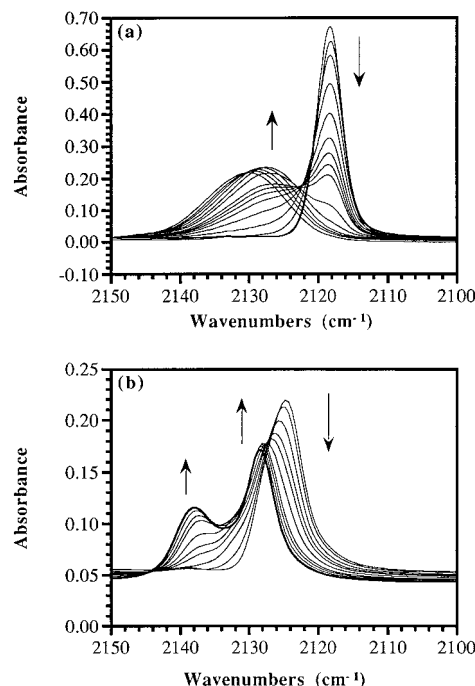


Figure 1. ATR-FTIR spectral studies in the $2100\text{--}2150\text{ cm}^{-1}$ region of films of (a) $[(n\text{-C}_4\text{H}_9)_4\text{N}]_2[\text{Pt}(\text{CN})_4]$ and (b) $[\text{Pt}(p\text{-CN-C}_6\text{H}_4\text{-C}_{10}\text{H}_{21})_4][\text{Pt}(\text{CN})_4]$ as the nitrogen inside the sample compartment is saturated with CH_3OH vapor. Arrows indicate the direction of change. Figure b is from ref 4b. Reprinted with permission. Copyright 1997 American Chemical Society.

$[(n\text{-C}_4\text{H}_9)_4\text{N}]_2[\text{Pt}(\text{CN})_4]$ and $[\text{Pt}(p\text{-CN-C}_6\text{H}_4\text{-C}_{10}\text{H}_{21})_4][\text{Pt}(\text{CN})_4]$. For the $[(n\text{-C}_4\text{H}_9)_4\text{N}]^+$ salt (Figure 1a), the $\nu(\text{CN})$ band of the dry film at 2118 cm^{-1} isospectically shifts to 2127 cm^{-1} . Once the 2118 cm^{-1} band has disappeared, another isospectical shift from 2127 to 2130 cm^{-1} is observed, indicating a second chemical transformation between the dry and CH_3OH -saturated film. At longer times, the $\nu(\text{CN})$ band remains at 2130 cm^{-1} but decreases in intensity. (For clarity, this is not shown in the figure.) This last change is probably due to the sorption of enough CH_3OH vapor to cause dissolution of the film and a decrease in the amount of contact between the solid-state chromophore and the ATR crystal surface.⁸ This spectroscopic behavior indicates that the cyanide ligands interact strongly with the $\text{CH}_3\text{-OH}$ vapor. Interactions of CH_3OH with the lone pair on the cyanide nitrogen atom polarize the $\text{C}\equiv\text{N}$ bond and increase the stretching frequency.⁵ Another effect of this interaction is to broaden the $\nu(\text{CN})$ band in a manner similar to what is observed in the IR spectra of alcohols.⁹ For the $[\text{Pt}(p\text{-CN-C}_6\text{H}_4\text{-C}_{10}\text{H}_{21})_4][\text{Pt}(\text{CN})_4]$ double-complex salt, a similar $\nu(\text{CN})$ shift is observed (Figure 1b). However the sorption of CH_3OH vapor, in this case, gives a CH_3OH -saturated film that exhibits two $\nu(\text{CN})$ bands instead of one. As described previously, this indicates that two different cyanide environ-

(8) We have observed that dissolution of a solid film on the surface of the ATR crystal causes a decrease in absorbance. This effect was previously attributed to a lower concentration of sample in contact with the crystal surface. See: (a) Ingle, J. D., Jr.; Crouch, S. R. *Spectrochemical Analysis*; Prentice Hall: Englewood Cliffs, NJ, 1988; pp 429–434. (b) Exstrom, C. L. Ph.D. Dissertation, University of Minnesota, 1995. Footnote 19 in ref 4b incorrectly describes this process as leading to an increase in absorbance.

(9) Pavia, D. L.; Lampman, G. M.; Kriz, G. S. *Introduction to Spectroscopy: A Guide for Students of Organic Chemistry*; Saunders College Publishers: PA, 1979.

(7) (a) Nagel, C. C.; U.S. Patent 4,834,909. (b) Miller, J. S.; Balch, A. L. *Inorg. Chem.* **1972**, *9*, 2069.

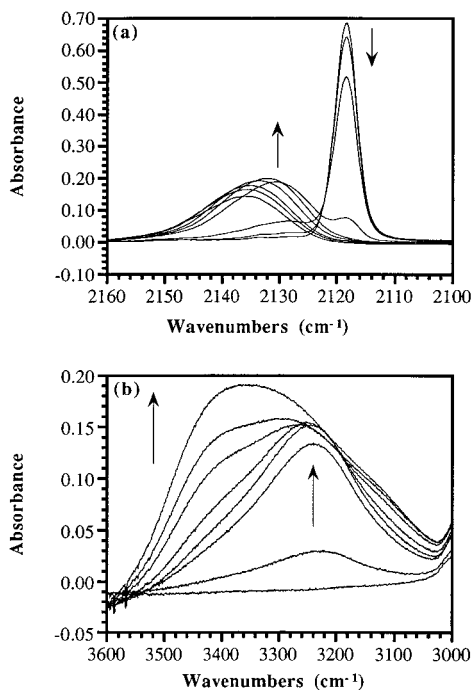


Figure 2. ATR-FTIR spectra studies in the (a) $\nu(\text{CN})$ and (b) $\nu(\text{OH})$ regions of a film of $[(n\text{-C}_4\text{H}_9)_4\text{N}]_2[\text{Pt}(\text{CN})_4]$ as the nitrogen inside the sample compartment is saturated with $\text{CF}_3\text{CH}_2\text{OH}$ vapor. Arrows indicate the direction of change.

ments per $[\text{Pt}(\text{CN})_4]^{2-}$ are present in the solid material.^{4b} Dissolution of the film is not observed, indicating that the CH_3OH vapor can penetrate the bulk solid despite the insolubility of the double-complex salt.

Table 1 shows the $\nu(\text{CN})$ band positions for $[(n\text{-C}_4\text{H}_9)_4\text{N}]_2[\text{Pt}(\text{CN})_4]$ and $[\text{Pt}(p\text{-CN-C}_6\text{H}_4\text{-C}_{10}\text{H}_{21})_4][\text{Pt}(\text{CN})_4]$ as a function of various VOC parameters. Interestingly, both $[(n\text{-C}_4\text{H}_9)_4\text{N}]_2[\text{Pt}(\text{CN})_4]$ and $[\text{Pt}(p\text{-CN-C}_6\text{H}_4\text{-C}_{10}\text{H}_{21})_4][\text{Pt}(\text{CN})_4]$ respond to VOC vapor in the infrared region. This indicates that the $\nu(\text{CN})$ stretch of the $[\text{Pt}(\text{CN})_4]^{2-}$ dianion responds to VOC vapors regardless of whether it is incorporated into an infinite stack as in the double-complex salt or present as loosely ordered chains as in the $[(n\text{-C}_4\text{H}_9)_4\text{N}]_2[\text{Pt}(\text{CN})_4]$ salt.^{8b} Vapochromic shifts range from 0 (H_2O , acetone) to 38 cm^{-1} (concentrated HCl) for $[(n\text{-C}_4\text{H}_9)_4\text{N}]_2[\text{Pt}(\text{CN})_4]$ and 0 (H_2O , hexanes) to 19 cm^{-1} (HCOOH) for $[\text{Pt}(p\text{-CN-C}_6\text{H}_4\text{-C}_{10}\text{H}_{21})_4][\text{Pt}(\text{CN})_4]$. One VOC that caused a dramatic $\nu(\text{CN})$ shift in both salts was $\text{CF}_3\text{CH}_2\text{OH}$. Because of highly electronegative fluorine atoms on the methyl group, the highly polar $\text{CF}_3\text{CH}_2\text{OH}$ forms strong hydrogen bonds with the cyanide ligands on the $[\text{Pt}(\text{CN})_4]^{2-}$ units. Dramatic changes in the $\nu(\text{OH})$ band were observed upon exposure of a film of $[(n\text{-C}_4\text{H}_9)_4\text{N}]_2[\text{Pt}(\text{CN})_4]$ to $\text{CF}_3\text{CH}_2\text{OH}$ vapor. As illustrated in Figure 2a the $\nu(\text{CN})$ for the cyanide anion shifts from a relatively sharp band at 2118 cm^{-1} to a broad band at 2134 cm^{-1} . Note that the last four spectra in Figure 2a show a maximum absorbance decrease from 0.18 to 0.13 while the $\nu(\text{CN})$ band position shifts only 1 cm^{-1} (from 2135 to 2136 cm^{-1}). Figure 2b shows the concurrent changes in the $\nu(\text{OH})$ region. Upon initial sorption of $\text{CF}_3\text{CH}_2\text{OH}$, a $\nu(\text{OH})$ band at 3250 cm^{-1} grows in intensity. This corresponds to the greatest change in the $\nu(\text{CN})$ band (2118 cm^{-1} shifts to 2134 cm^{-1}). Next, the $\nu(\text{OH})$ region (Figure 2b) shows no further increase in the 3250 cm^{-1} band intensity, but an additional

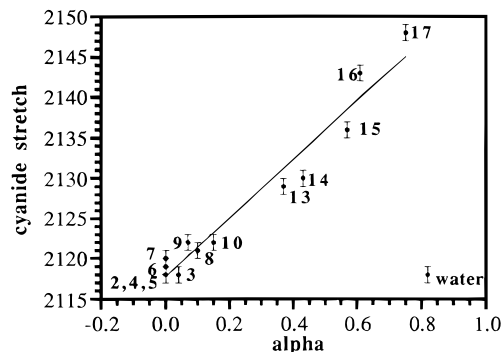


Figure 3. The $\nu(\text{CN})$ for $[(n\text{-C}_4\text{H}_9)_4\text{N}]_2[\text{Pt}(\text{CN})_4]$ plotted as a function of Abraham's α parameter. Numbers refer to VOCs listed in Table 1. The point for water is not included for the correlation line. The equation for the line is $y = 2117.8 + 36.387x$, $R = 0.97917$.

$\nu(\text{OH})$ band grows in intensity at approximately 3400 cm^{-1} . The last four spectra in both figures are characteristic of dissolution of the film in the $\text{CF}_3\text{CH}_2\text{OH}$. During this transition, the $\nu(\text{OH})$ band position is shifted 150 cm^{-1} toward higher energy relative to its previous position. This suggests that $\text{CF}_3\text{CH}_2\text{OH}$ undergoes two modes of hydrogen bonding. Initially, $\text{CF}_3\text{CH}_2\text{OH}$ -cyanide hydrogen bonds form resulting in an $\nu(\text{OH})$ band at 3250 cm^{-1} . Once the $[(n\text{-C}_4\text{H}_9)_4\text{N}]_2[\text{Pt}(\text{CN})_4]$ film is "saturated" with $\text{CF}_3\text{CH}_2\text{OH}$, further sorption results in dissolution of the film. During this conversion, $\text{CF}_3\text{CH}_2\text{OH}$ hydrogen bonds with itself, resulting in an $\nu(\text{OH})$ band shift to 3400 cm^{-1} . The ATR-IR spectrum of neat $\text{CF}_3\text{CH}_2\text{OH}$ shows a $\nu(\text{OH})$ band at 3390 cm^{-1} .

Initial attempts to correlate the $\nu(\text{CN})$ band position with various VOC physical properties or parameters were unsatisfying with the exception of Abraham's α parameter.^{12a} As seen in Figures 3 and 4, α (a measure of hydrogen bonding ability) correlates well with the cyanide stretching frequency in the infrared spectrum. For both salts, strong hydrogen-bonding VOCs (formic acid and acetic acid) give the highest cyanide stretching frequencies relative to the unexposed sample. Poor hydrogen-bonding VOCs (benzene and hexanes) give minimal changes in the cyanide stretching frequency. When the cyanide stretching frequency is plotted vs either $\text{p}K_a$ (in water) or gas-phase acidities, the correlation is much poorer. A direct comparison of the stretching frequencies for both complex salts shows that similar VOC-material interactions are present.

One solvent that does not correlate properly with α for either platinum compound is water. From the large α value of H_2O (0.82), one would predict that exposure of a $[(n\text{-C}_4\text{H}_9)_4\text{N}]_2[\text{Pt}(\text{CN})_4]$ or $[\text{Pt}(p\text{-CN-C}_6\text{H}_4\text{-C}_{10}\text{H}_{21})_4]$ -

(10) (a) March, J. *Advanced Organic Chemistry Reactions, Mechanisms, and Structure*, 4th ed.; Wiley and Sons: New York, 1992. (b) Reutov, O. A.; Beleskaya, I. P.; Butin, K. P. *CH-Acids*; Pergamon Press: New York, 1978. (c) Patai, S.; Rappoport, Z. *The Chemistry of Triple Bonded Functional Groups*; Wiley and Sons: New York, 1983. (d) Reeve, W.; Erikson, C. M.; Aluotto, P. F. *Can. J. Chem.* **1979**, *57*, 2747. (e) Pearson, D. *J. Am. Chem. Soc.* **1953**, *75*, 2439. (f) Arnett, E. M. *Prog. Phys. Org. Chem.* **1963**, *1*, 288.

(11) Lias, S. G.; Bartmess, J. E.; Liebman, J. F.; Holmes, J. L.; Levin, R. D.; Mallard, W. G. *J. Phys. Chem. Ref. Data* **1988**, *17*, Suppl. 1.

(12) (a) Abraham, M. H. *Chem. Soc. Rev.* **1993**, *73*. (b) Abraham, M. H.; Grellier, P. L.; Prior, D. V.; Duce, P. P. *Chem. Soc. Perkin Trans. II* **1989**, 699.

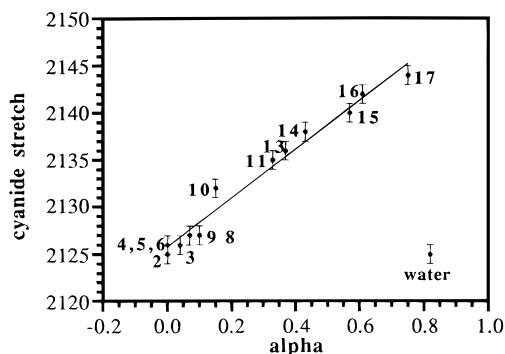


Figure 4. The $\nu(\text{CN})$ for $[\text{Pt}(p\text{-CN-C}_6\text{H}_4\text{-C}_{10}\text{H}_{21})_4][\text{Pt}(\text{CN})_4]$ plotted as a function of Abraham's α parameter. Numbers refer to VOCs listed in Table 1. The point for water is not included for the correlation line. The equation for the line is $y = 2125.8 + 25.882x$, $R = 0.98929$.

$[\text{Pt}(\text{CN})_4]$ film to H_2O would cause $\nu(\text{CN})$ shifts of approximately 30 and 22 cm^{-1} , respectively, but no shift was observed in either case. To rule out the possibility of the film being saturated with water prior to exposure, a sample of $[\text{Pt}(p\text{-CN-C}_6\text{H}_4\text{-C}_{10}\text{H}_{21})_4][\text{Pt}(\text{CN})_4]$ was dried in vacuo and then applied to the ATR crystal. After an initial spectrum was obtained, the film was saturated with water and then dried under a nitrogen purge for several days. Spectra taken throughout the experiment showed no change in $\nu(\text{CN})$ for the film. However, broad peaks due to $\nu(\text{OH})$ grew in during the exposure phase and slowly disappeared during the purge phase. This behavior indicates that water contacted the surface of the ATR crystal through gaps in the film rather than being incorporated into the film itself. We believe that the inability of water to penetrate the film is due to the presence of $[(n\text{-C}_4\text{H}_9)_4\text{N}]^+$ and $n\text{-C}_{10}\text{H}_{21}$ groups in the solid films. The networks of these long alkyl chains present hydrophobic barriers through which the water vapor is unable to pass. However, organic guest vapor can pass through these alkyl chain networks and interact with the $[\text{Pt}(\text{CN})_4]^{2-}$ ions. To test this hypothesis, a film of $[\text{Pt}(p\text{-CN-C}_6\text{H}_4\text{-CH}_3)_4][\text{Pt}(\text{CN})_4]$ (a much less lipophilic complex) was exposed to water vapor. This salt readily incorporates water and shows a large reversible shift in the $\nu(\text{CN})$ stretch. Further experiments are planned with this complex in the future.

To determine whether the mechanism(s) responsible for the vapochromic shifts in the IR and NIR for $[\text{Pt}(p\text{-CN-C}_6\text{H}_4\text{-C}_{10}\text{H}_{21})_4][\text{Pt}(\text{CN})_4]$ are related, we have plotted the previously collected NIR data against the same VOC parameters. Unfortunately, the correlations between NIR absorbance data and Abraham's α values, $\text{p}K_a$, or gas-phase acidity are more complex. The best of these are seen in Figure 5: a linear correlation exists between Abraham's α values and the NIR absorbance data for chloroform (10), isopropyl alcohol (11), ethanol (14), and methanol (15). However, other VOC vapors (such as hexanes (2), acetone(3), or dichloromethane (8)) with similar α values elicit dramatic shifts in NIR response.

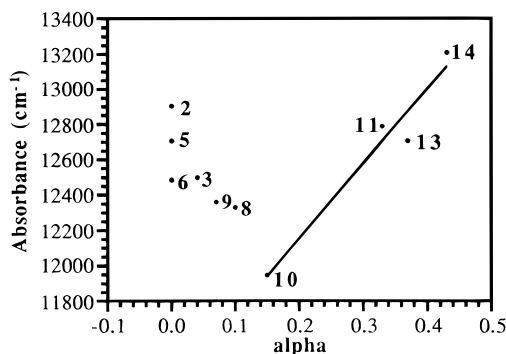


Figure 5. The energy in cm^{-1} of the NIR absorbance for $[\text{Pt}(p\text{-CN-C}_6\text{H}_4\text{-C}_{10}\text{H}_{21})_4][\text{Pt}(\text{CN})_4]$ plotted as a function of Abraham's α parameter. Numbers refer to VOCs listed in Table 1. The correlation line includes data points for α greater than 0.15. The equation for the line is $y = 11303 + 4248.7x$, $R = 0.97451$.

Clearly, the H-bonding mechanism that produces the infrared vapochromic shifts discussed here contribute to the NIR absorbance shifts reported previously for $[\text{Pt}(p\text{-CN-C}_6\text{H}_4\text{-C}_{10}\text{H}_{21})_4][\text{Pt}(\text{CN})_4]$ for VOCs with α values above 0.15, but for low α values one or more additional mechanisms are responsible for the NIR vapochromic effects.

Conclusions

The studies presented here indicate unequivocally that the $[\text{Pt}(\text{CN})_4]^{2-}$ dianion is a useful component for the construction of environmental sensor materials. It is also likely that other anionic cyanide complexes or complexes of other simple anions that retain a degree of basicity could also be used. The $\nu(\text{CN})$ stretch for both $[(n\text{-C}_4\text{H}_9)_4\text{N}]_2[\text{Pt}(\text{CN})_4]$ and $[\text{Pt}(p\text{-CN-C}_6\text{H}_4\text{-C}_{10}\text{H}_{21})_4][\text{Pt}(\text{CN})_4]$ show a high degree of correlation with Abraham's α values. It is clear that the $\nu(\text{CN})$ shifts observed in both of these salts are due to the hydrogen-bonding interactions between the VOC vapor and the cyanide ligands of the $[\text{Pt}(\text{CN})_4]^{2-}$ dianion. Further, because both complex salts respond in a similar fashion in the $\nu(\text{CN})$ region to VOC vapors, it is also apparent that the mechanism involved is not dependent upon the presence of an infinite stack of Pt centers. The complex correlation between the vapochromic shift in the NIR with either Abraham's α values, $\text{p}K_a$ (in H_2O), or gas-phase acidities for the VOCs suggests multiple mechanisms are responsible for the vapochromic activity of these double-salt complexes.

Acknowledgment. This work has been funded by the INEEL University Research Consortium. The INEEL is managed by Lockheed Martin Idaho Technologies Co. for the U.S. Department of Energy, Idaho Operations Office, under contract number DE-AC07-94ID13223. The FTIR spectrometer was purchased with funds from NSF Grant CHE-9307837.

CM970788T